

c. 3

ERIC-14 REPORT COLLECTION
**REPRODUCTION
COPY**

See Attached
Extra Sheet

*Analysis of Tritium Production
in Concentric Spheres of Oralloid and
⁶LiD Irradiated by 14-MeV Neutrons*

LOS ALAMOS NATIONAL LABORATORY
3 9338 00319 4627

Los Alamos

*Los Alamos National Laboratory is operated by the University of California for
the United States Department of Energy under contract W-7405-ENG-36.*

Photocomposition by Chris West

An Affirmative Action/Equal Opportunity Employer

This report was prepared as an account of work sponsored by an agency of the United States Government. Neither the United States Government nor any agency thereof, nor any of their employees, makes any warranty, express or implied, or assumes any legal liability or responsibility for the accuracy, completeness, or usefulness of any information, apparatus, product, or process disclosed, or represents that its use would not infringe privately owned rights. Reference herein to any specific commercial product, process, or service by trade name, trademark, manufacturer, or otherwise, does not necessarily constitute or imply its endorsement, recommendation, or favoring by the United States Government or any agency thereof. The views and opinions of authors expressed herein do not necessarily state or reflect those of the United States Government or any agency thereof.

ERRATA FOR LA-11110

Page 1 - Second line in introduction: ${}^6\text{Li}$ instead of ${}^9\text{Li}$.

Page 6 - Fourth line in first column: He instead of HE.

Page 6 - Fifth line from bottom, first column: fraction should be $\frac{dN}{dt}$ instead of $\frac{dn}{dt}$.

Page 7 - Last line of heading on fourth column, Table IV: should read (dps/sample) (add closing parenthesis).

Page 7 - Eleventh line from bottom, first column: σ_j instead of ϕ_j .

Page 8 - Sixth line from top, second column: σ_{Li6} instead of ϕ_{Li6} .

Page 8 - Seventh line from top, second column: σ_{Li7} instead of ϕ_{Li7} .

Page 9 - First line, first column: Table V instead of Table IV.

Page 13 - First sentence, first column, should begin: It is believed that the cause of poor tritium production results in ${}^7\text{Li}$ is.... (add the word "results.")

*Analysis of Tritium Production
in Concentric Spheres of Oralloid and
 ${}^6\text{LiD}$ Irradiated by 14-MeV Neutrons*

*L. Raymond Fawcett, Jr.**

*Roger R. Roberts II***

Raymond E. Hunter

**Collaborator at Los Alamos. Director of Physics and Pre-Engineering Programs,
Longwood College, Farmville, VA 23901.*

***Graduate Research Assistant at Los Alamos. Department of Physics,
Miami University, Oxford, Ohio 45056.*

LOS ALAMOS NATL. LAB. LIBS.



3 9338 00319 4627

CONTENTS

ABSTRACT	1
I. INTRODUCTION	1
II. EXPERIMENT	1
A. Source Neutrons	3
B. Enriched Uranium and ^6LiD Assembly	3
C. Tritium Production	3
D. Radiochemical Detector Foils	6
III. ANALYSIS	7
A. Tritium Production	7
B. Radiochemical Detector Foils	9
C. Perturbations	10
D. Errors	10
IV. RESULTS	10
A. Tritium Production	10
B. Radiochemical Detector Foils	11
1. (n,2n) Activation	11
2. (n,f) Activation	11
3. (n, γ) Activation	11
V. CONCLUSIONS	11
ACKNOWLEDGMENTS	16
APPENDIX A. Typical Tritium Production in ^7LiH Input File	20
APPENDIX B. Comparison of Tritium Production in ^7Li Samples with Cross Sections from ENDF/B-V vs. ENDF/B-V with ^{235}U Softened Fission Spectrum at High Energy	21
APPENDIX C. Comparison of Tritium Production in ^7Li Samples for Induced Background Originating from Ampule Quartz vs. Contaminated Helium	22
APPENDIX D. Comparison of Cross-Section Evaluations	23
REFERENCES	25

ANALYSIS OF TRITIUM PRODUCTION IN CONCENTRIC SPHERES OF ORALLOY AND ${}^6\text{LiD}$ IRRADIATED BY 14-MeV NEUTRONS

by

L. Raymond Fawcett, Jr., Roger R. Roberts II, and Raymond E. Hunter

ABSTRACT

Tritium production and activation of radiochemical detector foils in a sphere of ${}^6\text{LiD}$ with an oralloy core irradiated by a central source of 14-MeV neutrons have been calculated and compared with experimental measurements. The experimental assembly consisted of an oralloy sphere surrounded by three solid ${}^6\text{LiD}$ concentric shells with ampules of ${}^6\text{LiH}$ and ${}^7\text{LiH}$ and activation foils located in several positions throughout the assembly. The Los Alamos Monte Carlo Neutron Photon Transport Code (MCNP) was used to calculate neutron transport throughout the system, tritium production in the ampules, and foil activation. The overall experimentally observed-to-calculated ratios of tritium production were $0.996 \pm 2.5\%$ in ${}^6\text{Li}$ ampules and $0.903 \pm 5.2\%$ in ${}^7\text{Li}$ ampules. Observed-to-calculated ratios for foil activation are also presented.

I. INTRODUCTION

The objectives of this experiment were 1) to determine the integral of the ${}^6\text{Li}$ and ${}^7\text{Li}$ tritium production cross sections in a system composed of a ${}^6\text{LiD}$ -reflected enriched uranium sphere with a central source of 14-MeV neutrons and 2) to measure the transport of 14-MeV neutrons through the reflected assembly.

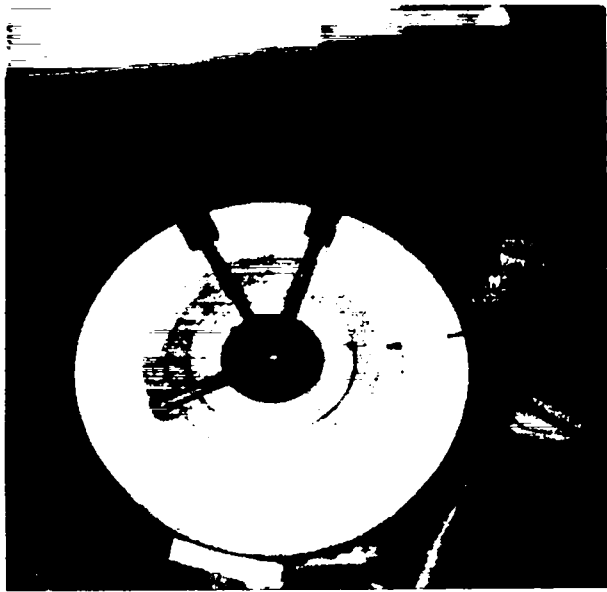
The experimental system was composed of a 15.23-cm-diam oralloy sphere (with channels to provide for a central 14-MeV neutron source) centered in a 60.0-cm-diam ${}^6\text{LiD}$ sphere consisting of a series of nested solid hemispherical shells (Figs. 1 a, b, and c). Integral determination of the neutron energy and flux as a function of distance from the center of the assembly was done by radiochemical detector foils placed inside the oralloy and between the ${}^6\text{LiD}$ shells at several distances from the source. Tritium production measurements were made with ${}^6\text{LiH}$ - and ${}^7\text{LiH}$ -filled quartz ampules placed in alcoves on and between the ${}^6\text{LiD}$

shells. Comparison of reaction rates determined by experiment and calculation tests the ability to calculate the integral over energy of the product of evaluated cross sections and calculated fluxes.

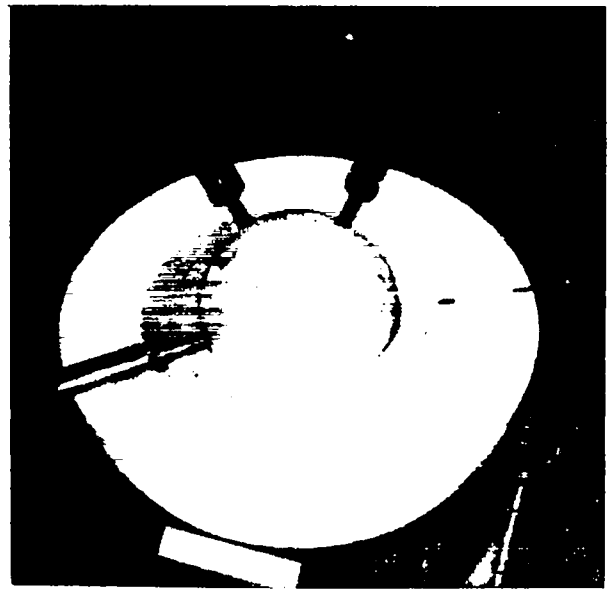
Although the experiment was performed in September 1977, measurements and calculation of the values of tritium production and radiochemical activation have just been completed.

II. EXPERIMENT

The following description of the experiment is taken predominately from three sources: an unpublished report by those who performed the experiment,¹ the experiment notebooks of A. Hemmendinger and C. E. Ragan, and a memorandum from J. S. Gilmore.²



(a)



(b)



(c)

Fig. 1. Bottom half of oralloy and ${}^6\text{LiD}$ assembly of hemishells is shown in (a). The tritium target is inside the steel ball at the center. Oralloy core and innermost ${}^6\text{LiD}$ shell completed are shown in (b). Top two outermost hemishells are missing. Almost complete experimental assembly is shown in (c). Top outermost hemishell is yet to be put in place.

A. Source Neutrons

Neutrons of 14 MeV were produced by 300-keV deuterons that were incident on a tritium target at the center of the experimental assembly. The assembly was exposed to 3.815×10^{15} 14-MeV source neutrons. The neutron source flux distribution for the same target setup used in this experiment has already been mapped over 4π sr for an earlier experiment.³ That distribution was used in the analysis of this experiment. A map of the flux distribution is in Fig. 3 of Ref. 3.

B. Enriched Uranium and ${}^6\text{LiD}$ Assembly

The enriched uranium consisted⁴ of two solid hemispherical shells of total mass 32.900 kg and isotopic composition 93.18 at.% ${}^{235}\text{U}$, 5.82 at.% ${}^{238}\text{U}$, and 1.00 at.% ${}^{234}\text{U}$. The ${}^6\text{LiD}$ was composed³ of six solid hemispherical shells of average density 0.7425 g/cm³ and isotopic composition 95.6 at.% ${}^6\text{Li}$ and 4.4 at.% ${}^7\text{Li}$. Both the uranium core and ${}^6\text{LiD}$ shells were machined so they could be fitted together to form a solid sphere, except for a small cavity at the center and three channels to house and access the tritium target. The dimensions and masses of the hemishells are in Table I. (The ${}^6\text{Li}$ specifications in Table I were extracted from Ref. 3, Part I, Table I.) Figs. 1 a, b, and c show the partially completed assembly.

C. Tritium Production

1. **Samples.** Tritium was produced in experimental samples through the reactions ${}^6\text{Li}(n,\alpha){}^3\text{H}$ and ${}^7\text{Li}(n,n'){}^4\text{He}$, ${}^3\text{H}$. The samples consisted of quartz ampules—some containing ${}^6\text{LiH}$, others ${}^7\text{LiH}$ —located in several positions throughout the ${}^6\text{LiD}$ sphere. Those at 30.0 cm from the center of the assembly had 0.032-in.-thick cadmium covers to absorb any room-return thermal neutrons. Information on ampule specifications and positions is in Table II. Although Table III of Ref. 1 places the innermost ampules at 7.6 cm from the center of the assembly, they were actually about 8.3 cm from the center. The oralloy sphere had an external radius of 7.62 cm. No alcoves were cut in the oralloy to accommodate ampules. The alcoves in the innermost ${}^6\text{LiD}$ shell were cut deeper and the ampules were taped below the surface of the ${}^6\text{LiD}$. The radii of these inner ampules were 0.50 cm; therefore, the distance from the assembly center to the ampule center was 8.3 ± 0.1 cm. Angular orientation of the ampules is shown in Fig. 2. The ampules were spherical with 1.0-mm-thick walls and had small stems on them for sealing after being loaded in a helium atmosphere.* (See Fig. 1 of Ref. 3 for a drawing of an ampule.) The ampules were not loaded with LiD because the tritium content in deuterium produced a dps background larger in most cases than that expected from tritium production in the ampules.

*LiH samples were prepared at Y-12 plant, Oak Ridge, TN.

TABLE I. Specifications for Hemispherical Shells

Material	Diameter (mm)		Mass (kg)
	Inside	Outside	
Oralloy	44.4	152.3	16.410
			16.339
			0.150 ^a
${}^6\text{LiD}$	154.3	252.0	2.465
			2.330
${}^6\text{LiD}$	254.0	400.0	9.133
			9.430
${}^6\text{LiD}$	402.0	600.0	30.000
			29.200

^aScrew and plugs.

TABLE II. LiH Sample Specifications

Li Isotope	Sample No.	Ampule Outside Radius (cm)	Distance From Source (cm)	Sample Mass ^a LiH (g)	
6	411	0.9	29.95	0.8381	
	412	0.9	29.95	0.9681	
	414	0.9	29.95	0.9073	
	410	0.9	20.15	0.9489	
	344	0.9	12.55	0.8912	
	346	0.9	12.75	0.8711	
	347	0.9	12.75	0.8966	
	338	0.5	8.37	0.1188	
	7	348	0.9	29.95	1.0542
		349	0.9	29.95	1.0200
		340	0.9	19.95	0.9464
		341	0.9	19.95	0.9502
		342	0.9	20.15	1.0104
401		0.9	12.55	1.0398	
407		0.9	12.75	0.9267	
408		0.9	12.55	0.9454	
355		0.5	8.22	0.1398	
339		0.5	8.37	0.1210	

^aTaken from F. D. Bender, Document Transmittal Form, "Ampule Data," June 27, 1977. Available from L. R. Fawcett, Jr.

After irradiation, the LiH ampules were assayed for tritium content by Teledyne Isotopes, Westwood, NJ 07675. The amount of tritium produced in each sample was measured at Teledyne by proportional counter and by liquid scintillator. All results were then corrected for radioactive decay of tritium to September 20, 1977. Finally, the Teledyne count rates were normalized to thermal-neutron tritium-production results³ based on the ratio of the thermal capture cross section of ⁶Li to that of ¹⁹⁷Au. The result was that Teledyne's net counting rate was divided by 1.058 for large ampules and by 1.103 for small ampules.

2. Background. Before normalization, both natural and induced backgrounds were subtracted from

Teledyne's measured counting rates. The backgrounds in unirradiated LiH samples are shown in Table III.* The induced background was measured by irradiating helium-filled ampules along with the LiH samples at the time of the experiment. Induced background had a significant impact on the ⁷Li part of the experiment because it was greater than 50% of the measured counting rate for small ampules. The large induced

*The information in this table is similar to that in Table II of Ref. 1, with one major exception. Ampule 349, an irradiated sample, was mistakenly included in Table II of Ref. 1 as an unirradiated sample. Ampule 349 is correctly excluded from Table III of this work. Therefore, the ⁷Li average background is corrected from $3.88 \text{ s}^{-1}\text{g}^{-1}$ to $2.69 \text{ s}^{-1}\text{g}^{-1}$.

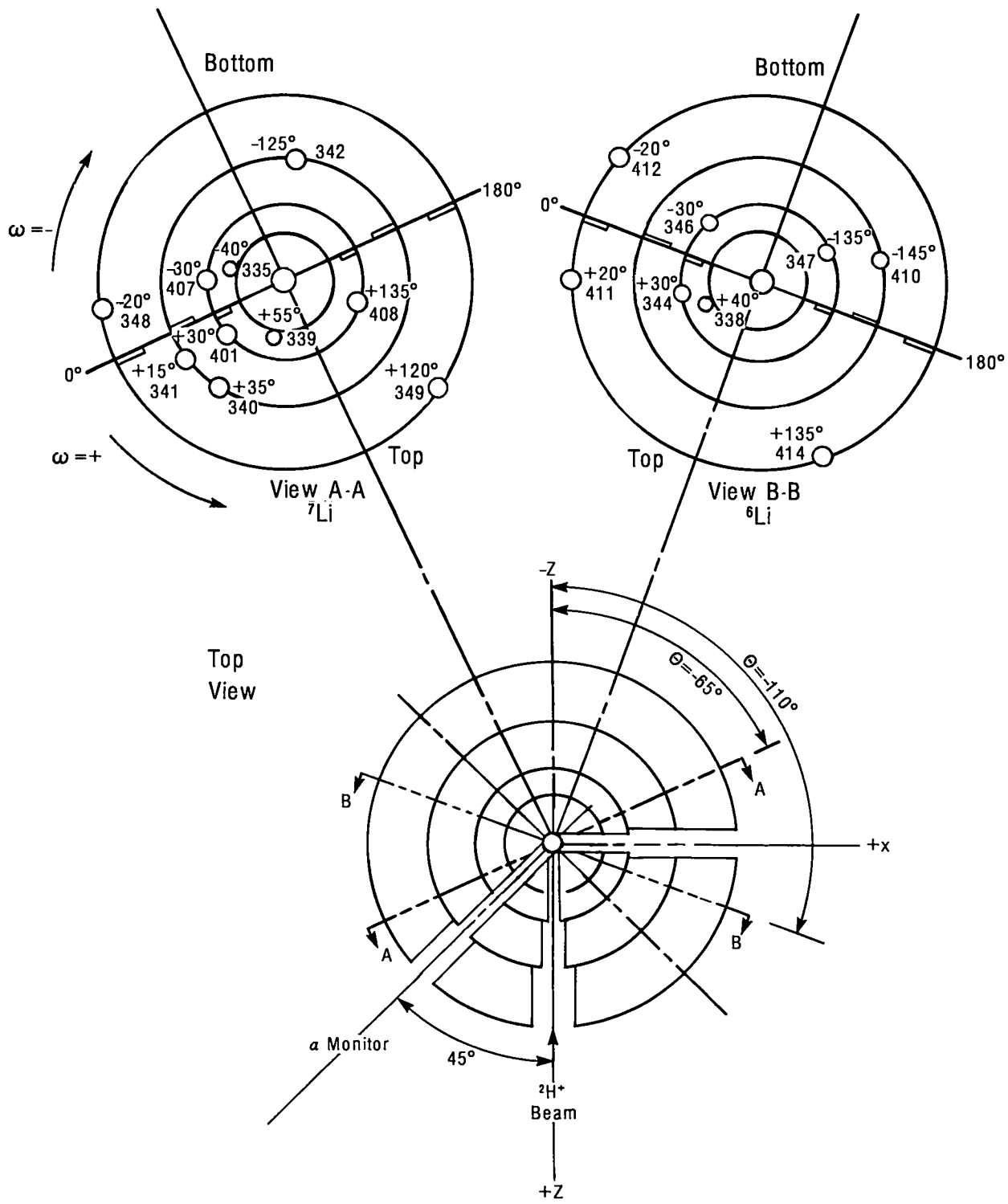


Fig. 2. Orientation of ampules with respect to ${}^2\text{H}^+$ beam. In views A-A and B-B, top and bottom refer to the assembly at the time of the experiment.

TABLE III. Tritium Backgrounds in LiH Samples (Unirradiated)

Isotope	Sample No.	Background ($s^{-1} g^{-1}$)
${}^6\text{Li}$	417	0.273 ± 0.11
	418	0.247 ± 0.11
	Av.	0.260 ± 0.07
${}^7\text{Li}$	343	2.93 ± 0.18
	413	2.35 ± 0.15
	416	2.78 ± 0.17
	Av.	2.69 ± 0.10

background is particularly worrisome since in the 14-MeV experiment (Ref. 3) this same measurement was small enough to be neglected. The experimenters say "there must have been some contaminant in the H_2 (loading atmosphere) whose reaction product was carried through the chemical processing."¹ The induced background data are in Table IV.

3. Absolute Tritium Production. The absolute tritium production for each ampule is presented in Table V (Results section). Absolute tritium production is calculated from the experimentally determined normalized net counting rate by

$$N(\text{obs}) = \frac{N}{M} = \frac{1}{\lambda M} \cdot \frac{dN}{dt}, \quad (1)$$

where

$N(\text{obs})$ is the number of tritons produced per lithium atom in the sample by the total number of source neutrons; that is, the absolute tritium production,

N is the number of tritium atoms present per gram of LiH,

$\frac{dN}{dt}$ is the normalized net counting rate ($s^{-1} g^{-1}$),

M is $8.520 \times 10^{22} {}^6\text{LiH} g^{-1}$ and $7.506 \times 10^{22} {}^7\text{LiH} g^{-1}$,

$\lambda = 1.7781 \times 10^{-9} s^{-1}$

Ampules 401, 407, and 408 were all at the same distance from the central neutron source. However, their experimental values of tritium production vary by a factor of 2. The experimenters state¹ that there is something wrong with the results from those three samples.

D. Radiochemical Detector Foils

Six packets of radiochemical detector foils were placed in a plane through the center of the assembly at 90° to the incident deuteron beam. One packet was on the exterior surface of the largest ${}^6\text{LiD}$ shell at 30.0 cm from the center of the assembly; two packets were between ${}^6\text{LiD}$ shell interfaces at 20.0 and 12.6 cm from the center; one packet was at the oralloy/ ${}^6\text{LiD}$ interface at 7.5 cm from the center; and two packets were within the oralloy core at 4.8 and 2.3 cm from the center.² A 0.5-in.-diam radial channel in the lower oralloy hemisphere directly below and at 60° to the cooling channel had been cut to house foil packets. This channel was completely backfilled with solid oralloy plugs after the foils were inserted. The several foil locations are shown in Fig. 3. The foil nuclides were ${}^{45}\text{Sc}$, ${}^{58}\text{Ni}$, ${}^{89}\text{Y}$, ${}^{90}\text{Zr}$, ${}^{169}\text{Tm}$, ${}^{191}\text{Ir}$, ${}^{193}\text{Ir}$, ${}^{197}\text{Au}$, ${}^{235}\text{U}$, and ${}^{238}\text{U}$. A complete description of the foils is in Ref. 2.

TABLE IV. Induced Background in He-Filled Ampules (Irradiated)

Isotope ^a Plane	Distance From Source (cm)	Sample No.	Ampule Size	Induced ^b Background (dps/sample)
⁶ Li	30.0	423, 424	Large	0.233
	20.0	404, 405	Large	4.38
	12.6	160, 402	Large	17.98
	8.3	331	Small	27.00
⁷ Li	30.0	421, 422	Large	0.17
	20.0	426	Large	4.97
	12.6	403, 427	Large	14.5
	8.3	333	Small	40.5

^aAll ⁶LiH ampules and corresponding He filled ampules were placed in one plane in the experimental assembly; all ⁷LiH and corresponding He ampules were placed in another.

^bTaken from Ref. 1, Table III.

III. ANALYSIS

The Los Alamos Monte Carlo Neutron Photon Transport Code (MCNP)⁵ was used to calculate neutron transport in the enriched uranium core and the ⁶LiD. MCNP also calculated tritium production in the ampules and foil activation through

$$\int \phi_i(E)\sigma_j(E)dE, \quad (2)$$

where

ϕ_i is the neutron fluence (in neutrons $\text{cm}^{-2}\text{MeV}^{-1}$) at ampule or foil position i , and

σ_j is the reaction cross section for reaction j .

The geometry of the oralloy hemispheres was modeled according to the specifications contained on an engineering drawing⁶ of the core, and that of the ⁶LiD shells was modeled according to the information contained in Table I. Three radial channels were cut into the oralloy and ⁶LiD shells to accommodate an α monitor, the ²H⁺ beam, and cooling tubes. These channels were included in the MCNP model.

The neutron multiplication of the system exceeded 20. This made it difficult to keep MCNP running be-

cause some histories required more than 20 s to complete. To make calculations, some artificial cutoffs were required in the input files. Even then the problems ran very slowly. Many runs required more than 20 h computer time.

A. Tritium Production

All tritium production calculations were three dimensional, with each ampule modeled in the MCNP input file at the position where it was located in the experimental assembly. Track length per unit volume tallies were used. A typical input file is attached as Appendix A. Although the spherical ampules had stems, they were treated as spheres without stems to simplify the model. The ampule radii used in the calculations (0.50 cm for small and 0.90 cm for large ampules) matched the outside rather than inside diameter to make an approximate allowance for stem volume. Cadmium covers of 0.032 in. were modeled on all ampules at 30.0 cm. The correct mass of LiH was modeled in each ampule. The correct mass was particularly important to account properly for the "flux trap" effect discussed on page 7 of Ref. 7.

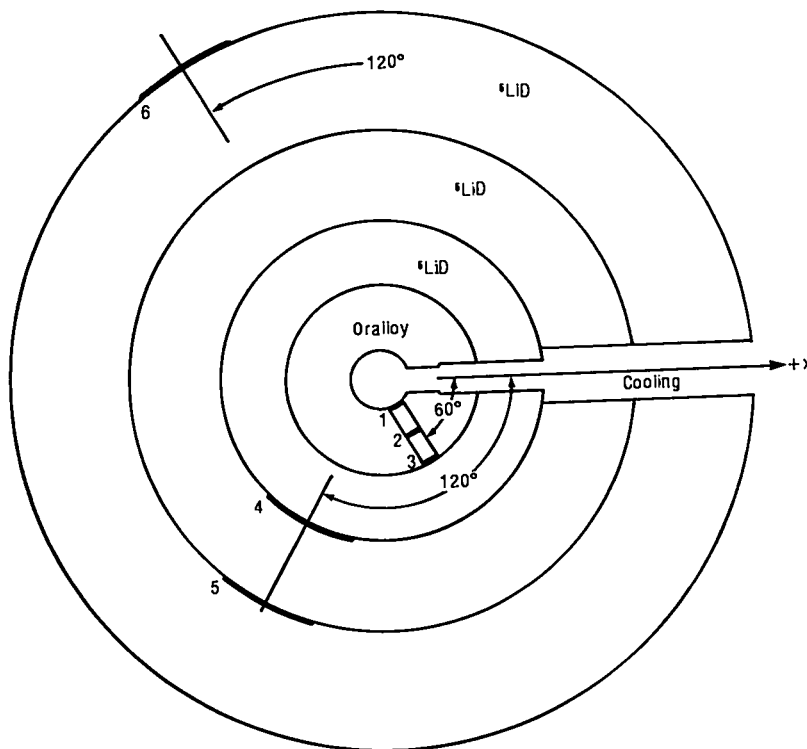


Fig. 3. Orientation of foils. Foils were located in a vertical plane through the center of the assembly and perpendicular to the $^2\text{H}^+$ beam. The numbers 1 through 6 locate the foil packets.

The cross sections used for both neutron transport and tritium production were from the ENDF/B-V evaluation.*

Since all ampules contained a mixture of ^6LiH and ^7LiH , tritium production in an ampule had to be calculated as the sum of two integrals as follows:

$$t \text{ prod. } ^6\text{Li} = 0.9590 \int \phi_i(E) \bar{\sigma}_{^6\text{Li}}(E) dE + 0.0410 \int \phi_i(E) \bar{\sigma}_{^7\text{Li}}(E) dE \quad (3)$$

*ENDF/B-V cross sections were used for transport and tritium production, except for ^2H and ^7Li , for which the 1982 Los Alamos Group T-2 evaluations were employed. The Group T-2 evaluation for ^7Li is the same as ENDF/B-V Revision 2. The ^2H evaluation is the same as ENDF/B-V except the library used here has been updated with correlated energy angular distribution for the (n,2n) reaction.

$$t \text{ prod. } ^7\text{Li} = 0.001 \int \phi_i(E) \phi_{^6\text{Li}}(E) dE + 0.999 \int \phi_i(E) \sigma_{^7\text{Li}}(E) dE, \quad (4)$$

where

- $\phi_i(E)$ is the average neutron fluence over the volume of ampule i ,
- $\phi_{^6\text{Li}}$ is the reaction cross section for $^6\text{Li}(n,\alpha)$, and
- $\phi_{^7\text{Li}}$ is the reaction cross section for $^7\text{Li}(n,n'\alpha)$.

The observed (experimental) values of absolute tritium production were derived from the Net Counting Rate Normalized column of Table III, Ref. 1, using Eq.(1). The values of the normalized net counting rate for ^7Li were adjusted for a natural background of $2.69 \pm .095 \text{ s}^{-1} \text{ g}^{-1}$ from the original, incorrect $3.88 \pm 1.13 \text{ s}^{-1} \text{ g}^{-1}$.

In Table IV one finds that although the observed-to-calculated (O/C) ratios for tritium generation in ${}^7\text{Li}$ are generally not very good, for ampules 335 and 339 the ratios are totally unacceptable in that the experimental values are about half as large as the calculated values.

Since the ${}^7\text{Li}$ tritium-production cross section has a threshold of about 2.8 MeV, and ampules 335 and 339 are directly exposed to the fission neutrons from the oralloy ball, it was thought that possibly the high-energy end of the ENDF/B-V ${}^{235}\text{U}$ fission spectrum is too hard. To test the effect of a softer fission tail, R. C. Little and R. E. Seamon⁸ modified the ENDF/B-V ${}^{235}\text{U}$ cross section file so that it contained a fission spectrum whose high-energy tail at $E' = 5.0$ MeV was reduced to 50% of that of ENDF/B-IV and at $E' = 12$ MeV was reduced to 10% of that of ENDF/B-IV. This modified fission spectrum greatly improved the observed-to-calculated ratios for ampules 335 and 339 but also produced lower calculated values in the other ${}^7\text{Li}$ ampules. The results are presented in Appendix B.

As mentioned in Section II.C.2 on background, the experimenters felt there must have been a contaminant that could be activated in the helium atmosphere in which the ampules were loaded. If it is assumed that the induced background count rate in Table IV is produced totally by a reaction product in contaminated helium, the observed values of tritium production can be properly adjusted. First the free volume of a loaded ampule is calculated by subtracting the LiH volume from the ampule volume. Assume the free volume to be completely filled with helium (since loading occurred in a helium atmosphere). Then the fraction of volume occupied by helium will be equal to the fraction of the induced background measurement (in the corresponding helium-filled ampule) that must be subtracted from the measured counting rate (less natural background). For example, the induced background for ${}^7\text{Li}$ at 8.3 cm in a helium-filled ampule was measured to be $40.5 \frac{\text{dis}}{\text{s}}$. In ampule 339 the volume of helium is 58.4%. Therefore, the induced background in 339 is $(40.5 \frac{\text{dis}}{\text{s}})(0.584) = 23.7 \frac{\text{dis}}{\text{s}}$.

The measured counting rate (less natural background) was $540.6 \text{ dis/s} - g$. Therefore, the net counting rate is given by

$$\frac{(540.6 \text{ dis s}^{-1}g^{-1})(0.121 \text{ g}) - 23.7 \text{dis s}^{-1}}{0.121 \text{ g}} = 345 \text{ dis s}^{-1}g^{-1}$$

rather than $205 \text{ dis s}^{-1}g^{-1}$, as is the case when the induced background is assumed to originate in the glass of the ampule.

Based on this helium contamination assumption, the O/C ratios for ampules 335 and 339 are substantially improved without much detriment to the other ${}^7\text{Li}$ O/C ratios. The results are presented in Appendix C.

B. Radiochemical Detector Foils

The radiochemical activation calculations were three dimensional (using point detectors) for foil positions 1, 2, and 3 inside the oralloy, and one dimensional (using surface tallies) for foil positions 4, 5, and 6 in and on the ${}^6\text{LiD}$. Of course, one would prefer to use the three-dimensional model for all foil positions. However, the point detectors require prohibitive amounts of computer time to produce good statistics in a low-flux environment.

The one-dimensional calculation is thought to be justified on the premise that outside the oralloy the neutron fluence approaches isotropy.

Point detectors, which were modeled in the input file at the experimental coordinates of the foils, tally the neutron fluence at the detector location. A surface tally produces an integrated fluence over an entire surface.

Evaluated dosimetry/activation cross sections for some foil nuclides were available from several sources.⁹ In such cases the choice of dosimetry cross section was based on the advice of the authors of Ref. 9. The cross sections used for each nuclide and reaction are identified in Tables VII and VIII in the Results section. The cross sections used for neutron transport were taken from the ENDF/B-V evaluation.

Because the observed-to-calculated ratios for the radiochemical detector foils are in some cases unacceptable, the calculated values were redone using a ${}^{235}\text{U}$ transport cross section with modified fission spectrum, as described in Section III.A and Ref. 8. This modification was expected to decrease calculated activation in (n,2n) reactions which would produce observed-to-calculated ratios closer to unity. Although the modified ${}^{235}\text{U}$ transport cross section did in fact improve O/C ratios for (n,2n) reactions, it caused significant deterioration in the ratios for (n, γ) and (n,f) reactions.

C. Perturbations

The effects of several undesirable physical phenomena are inextricably woven into the experimental results. Although two of these phenomena will be mentioned, their influences on the experiment are thought to be small enough not to warrant further investigation.

One of these phenomena is room return. The experiment was performed in a large steel and concrete room. In the ${}^6\text{LiD}$ core experiment (Ref. 7), which took place in the same room, the influence of room return on radiochemical activation foils was investigated in some detail. In all cases room return contributed less than 1% of induced foil activity. Since in this experiment the outer ampules had cadmium covers, it is expected that tritium production caused by room return was negligible. Another phenomenon during the experiment was self- and cross-activation of the foils. Inside the oralloy core the foils were packaged on top of one another. Thus not only would there be self-activation of a foil from neutrons born within it, but also cross-activation from neutrons born in the superimposed foils penetrating the first foil. Self- and cross-activation were investigated in Ref. 7. The largest combined effect found there was 1.9% of the total activation from all other neutrons. This was for the ${}^{238}\text{U}(n,\gamma)$ reaction. For all other reactions the effect was much smaller. Therefore, the calculated activation values in this experiment are not corrected for self- and cross-activation.

D. Errors

Tallies calculated by the MCNP transport code are accompanied by a statistical error of one fractional standard deviation of the mean. No estimates of cross-section uncertainties are included. The precisions of the experimental values for the foils were taken from Table 1 of Ref. 2. The precisions of the experimental values for tritium production are given in Ref. 1. These are the uncertainties assigned to the observed and calculated values found in Tables V, VII, and VIII (Results section). In addition, for tritium production the experimenters estimated a systematic error of less than 6%. Generally the errors quoted on observed-to-calculated ratios are for one fractional standard deviation and consist of the square root of the sum of the squared experimental and calculated fractional errors. When uncertainties were derived by other formulations, the method is explained by footnotes to the tables.

IV. RESULTS

A. Tritium Production

Table V lists the tritium production for each ampule and the corresponding observed-to-calculated ratios. Whereas specific tritium production, $f(r)$, is reported in Ref. 1, Table III, the absolute tritium production, $N(\text{obs})$, is reported here. Absolute tritium production is defined as the number of tritons produced per lithium atom in an ampule for the total number of source neutrons. Specific and absolute tritium production are related by

$$N(\text{obs}) = \frac{f(r)n}{4\pi r^2}, \quad (5)$$

where

$$f(r) \text{ is in units of } \frac{\text{tritons produced} \cdot \text{mm}^2}{\text{Li atom} \cdot \text{source neutron}}$$

where

n is the number of source neutrons, and
 r is the distance from the neutron source to the center of an ampule in millimeters.

The calculated tritium production in ${}^6\text{Li}$ ampules matches the experimentally measured values quite well. Experimentally observed-to-calculated ratios lie between 0.87 to 1.09, with several ratios very near unity. Observed-to-calculated ratios are unity within the limits of the quoted uncertainties for six of eight ampules.

The observed-to-calculated ratios of tritium production in several of the ${}^7\text{Li}$ ampules are unacceptable. For ampules in the 20.0-cm and 30.0-cm radial positions, the results, although not good, are at least marginally acceptable. Only observed and calculated values are presented at the 12.6-cm radial position. Here the large discrepancy between observed values (approximately 100% from smallest to largest) appears to be due to some unknown experimental problem. As mentioned earlier, the experimenters comment in their report¹ that there is obviously something wrong with the measured values from ampules 401, 407, and 408. It should be noted that in the tritium assay, the ampules were destroyed, so the source of the discrepancy cannot be determined. The results from ampules 335 and 339 in the 8.3-cm position are totally unacceptable. Here the experimentally observed values are only approximately 50% of the calculated values.

The experimenters' comment in Ref. 1 about induced activity in contaminated helium prompted calculation of the influence contaminated helium may

TABLE V. Tritium Production—Observed and Calculated^a

Li Isotope	Sample No.	Location		$N(\text{Obs})^c \times 10^{13}$	$N(\text{Calc})^d \times 10^{13}$	Observed ^e Calculated	
		r (mm)	ω^b (deg)	$\left(\frac{\text{Tritons Produced}}{\text{Li Atom}} \right)$	$\left(\frac{\text{Tritons Produced}}{\text{Li Atom}} \right)$		
6	411	299.5	20	$8.495 \pm 6\%$	$7.763 \pm 6\%$	$1.094 \pm 9\%$	
	412	299.5	-20	$9.104 \pm 6\%$	$9.003 \pm 9\%$	$1.011 \pm 10\%$	
	414	299.5	135	$9.375 \pm 6\%$	$8.820 \pm 7\%$	$1.063 \pm 9\%$	
	410	201.5	-145	$96.16 \pm 6\%$	$97.20 \pm 3\%$	$0.989 \pm 7\%$	
	344	125.5	30	$453.0 \pm 6\%$	$481.7 \pm 2\%$	$0.940 \pm 6\%$	
	346	127.5	-30	$468.7 \pm 6\%$	$453.6 \pm 2\%$	$1.033 \pm 6\%$	
	347	127.5	-135	$451.1 \pm 6\%$	$467.0 \pm 2\%$	$0.966 \pm 6\%$	
	338	83.7	40	$1004 \pm 6\%$	$1153 \pm 2\%$	$0.872 \pm 6\%$	
	7	348	299.5	-20	$0.336 \pm 18\%$	$0.378 \pm 12\%$	$0.889 \pm 22\%$
		349	299.5	120	$0.328 \pm 20\%$	$0.240 \pm 13\%$	$1.367 \pm 24\%$
340		199.5	35	$1.618 \pm 8\%$	$1.49 \pm 7\%$	$1.086 \pm 11\%$	
341		199.5	15	$1.551 \pm 9\%$	$1.84 \pm 7\%$	$0.843 \pm 11\%$	
342		201.5	-125	$1.618 \pm 9\%$	$1.42 \pm 8\%$	$1.139 \pm 12\%$	
401		125.5	30	$9.613 \pm 5\%$	$7.42 \pm 3\%$		
407		127.5	-30	$14.71 \pm 5\%$	$7.09 \pm 3\%$		
408		125.5	135	$7.410 \pm 7\%$	$7.13 \pm 3\%$		
335		82.2	-40	$14.21 \pm 14\%$	$30.1 \pm 3\%$	$0.472 \pm 14\%$	
339		83.7	55	$14.01 \pm 16\%$	$26.7 \pm 3\%$	$0.525 \pm 16\%$	

^aThe quoted uncertainties on both observed and calculated values are for one fractional standard deviation. In addition, there is an estimated <6% systematic error in the observed values which is not included in the errors quoted here.

^bAngles above the parting plane in the experimental configuration are positive; angles below the parting plane are negative.

^cObserved tritium production extracted from Ref. 1, Table III. (Tritons produced per Li atom in an ampule from 3.815×10^{15} source neutrons.)

^dTritium production calculated in this work using ENDF/B-V cross section data for both transport and tritium production. (Tritons produced per lithium atom in an ampule from 3.815×10^{15} source neutrons.)

^eThe quoted errors were determined from a square root of the sum of the squares combination of the observed and calculated uncertainties.

have had on the observed count rate - hence, tritium production. These results are presented in Appendix C. Clearly, if the induced background (which was, for ampoules 335 and 339, greater than 50% of the measured counting rate) did result from contaminated helium, the observed-to-calculated ratios in ampoules 335 and 339 are dramatically improved without substantial negative effect on the other ${}^7\text{Li}$ ratios. Induced activity by contaminated helium would have a negligible effect on the observed tritium production in ${}^6\text{Li}$ because the measured counting rate is hundreds of times larger than the fraction of induced background that could be attributed to activation of contaminated helium.

The overall observed-to-calculated tritium production ratio was obtained by equal-weight averaging of ratios for each isotope. The average ratio for ${}^6\text{Li}$ (including all ampoules) is

$$\overline{(\text{Obs}/\text{Calc})}_t \text{ prod. in } {}^6\text{Li} = 0.996 \pm 2.5 \%^*$$

The average ratio for ${}^7\text{Li}$ (excluding ampoules 401, 407, and 408) is

$$\overline{(\text{Obs}/\text{Calc})}_t \text{ prod. in } {}^7\text{Li} = 0.903 \pm 5.2 \%^*$$

The information in Table V is summarized in Table VI by presenting the average tritium production at each radius. The observed-to-calculated ratios for ${}^6\text{Li}$ range between 0.871 and 1.05. For ${}^7\text{Li}$ they lie between 0.497 and 1.07. The O/C ratios are unity within the limits of the quoted uncertainties in four of seven cases for the two nuclides.

B. Radiochemical Detector Foils

Table VII contains the experimentally observed and calculated values of radiochemical activation. Table VIII is more interesting because the experimental results are compared with calculated values through observed-to-calculated ratios. It appears that, except for six or seven commonly well-known dosimetry cross sections such as ${}^{197}\text{Au}(n,\gamma)$ and ${}^{235}\text{U}(n,f)$, a number of less well-known cross-section evaluations are in error. The dosimetry cross sections were taken from several sources, as described in footnote c of Tables VII and

VIII. Approximately 2/3 of the observed-to-calculated ratios differ from unity by more than 10%, and a few differ by a factor of 3. It is believed that this information will be useful to those who participate in determining recommended cross sections.

Figures 4a through 4q are graphs of the ratios in Table VIII. Specific comments on comparisons of the various evaluations from Ref. 7 and this paper are given in Appendix D.

1. (n,2n) Activation. Except for ${}^{89}\text{Y}(n,2n)$, the calculated induced activity is greater than that observed. The lack of a consistent pattern of increasing or decreasing ratio magnitudes with increasing radius does not suggest a code transport difficulty but implies uncertainty in the dosimetry cross sections.

2. (n,f) Activation. Both the ${}^{235}\text{U}(n,f)$ and the ${}^{238}\text{U}(n,f)$ cross sections are well known. Yet at all radii for both reactions the calculated activity is an average of about 12% greater than that observed. Again the ratio magnitude shows no pattern of increasing or decreasing with increasing distance from the source, implying reliable neutron transport calculations.

3. (n, γ) Activation. Here only ${}^{89}\text{Y}(n,\gamma)$, ${}^{193}\text{Ir}(n,\gamma)$, and ${}^{197}\text{Au}(n,\gamma)$ results are acceptable. One would also have expected the ${}^{238}\text{U}(n,\gamma)$ ratios to be close to unity because the ${}^{238}\text{U}(n,\gamma)$ capture cross section should be reasonably well known up to 2 MeV in any dosimetry evaluation. Such apparently is not the case. In the 20.0- and 30.0-cm radius positions, experimentally determined activities exceeded calculated values by almost two to one. The ${}^{45}\text{Sc}(n,\gamma)$ and ${}^{169}\text{Tm}(n,\gamma)$ ratios are unacceptable. It is thought that this is because their (n, γ) cross sections are not as generally well known as are those of ${}^{89}\text{Y}$, ${}^{193}\text{Ir}$, and ${}^{197}\text{Au}$.

V. CONCLUSIONS

Experimentally observed and calculated values for tritium production in ${}^6\text{Li}$ match quite well. As noted earlier, the observed-to-calculated ratios for tritium production in ${}^7\text{Li}$ were marginally acceptable only in the two regions of deepest penetration and unacceptable elsewhere. The results from the radiochemical activation part of this experiment will most profitably be used as feedback for those who recommend dosimetry cross sections.

*This uncertainty does not include any estimate of systematic error.

It is believed that the cause of poor tritium production in ${}^7\text{Li}$ is that most of the ${}^7\text{Li}$ experimental values have significant problems associated with them. Those we know about are listed below.

1. An irradiated ampule was included in a group of unirradiated ampules from which natural background was determined. (It is believed that this problem has been corrected by removal of the irradiated ampule from the natural background data base.)
2. The irradiated ampules used to measure induced background may have contained contaminated helium whose reaction product produced a count rate greater than that due to tritium produced in ampules 335 and 339. There appears to be no way at this point to determine what portion of induced background came from helium and what portion was due to activated impurities in ampule quartz. Without this knowledge the experimental value of net counting rate cannot be determined correctly.
3. The experimenters contend that there is obviously something wrong with the measured results from ampules 401, 407, and 408 in that the net count rate per gram of ${}^7\text{Li}$ from 407 was twice that of 408 and these ampules were all 12.6 cm from the neutron source, where the neutron fluences to which they were exposed should have been comparable.
4. The experimental error associated with ampules 348 and 349 is unacceptably large.

TABLE VI. Average Tritium Production at Each Radius Observed and Calculated^a

Li Isotope	Distance from Source (mm)	$N(\text{Obs})^{b,c} \times 10^{13}$	$N(\text{Calc})^{c,d} \times 10^{13}$	Observed ^e Calculated
		Experiment (Tritons Produced) Li Atom	Calculated (Tritons Produced) Li Atom	
6	300	8.991 ± 3%	8.529 ± 4%	1.054 ± 5%
	200	96.16 ± 6%	97.20 ± 3%	0.989 ± 7%
	127	457.6 ± 3%	467.4 ± 1%	0.979 ± 3%
	83	1004. ± 6%	1153. ± 2%	0.871 ± 6%
7	300	0.332 ± 13%	0.309 ± 9%	1.074 ± 16%
	200	1.596 ± 5%	1.583 ± 4%	1.008 ± 6%
	127	10.58	7.213 ± 2%	
	83	14.11 ± 11%	28.40 ± 2%	0.497 ± 11%

^aThe quoted uncertainties on both observed and calculated values are for one fractional standard deviation. In addition, there is a less than 6% systematic error in the observed values.

^bObserved tritium production (tritons produced per lithium atom from 3.81×10^{15} source neutrons).

^cThe errors assigned to the observed and calculated averages were determined by:

$$s = \left(\frac{1}{\sum \frac{1}{s_i^2}} \right)^{1/2}$$

^dTritium production calculated in this work using ENDF/B-V cross-section data for both transport and tritium production. (Tritons produced per lithium atom from 3.18×10^{15} source neutrons.)

^eThe quoted errors were determined from a square root of the sum of the squares combination of the observed and calculated uncertainties.

TABLE VII. Experimental^a and Calculated Values ($\times 10^{13}$) for Activation of Detector Foils (ENDF/B-V Transport Sections)

Reaction	Activation ^{b,c}		Distance from Source (cm)					
	Cross Section	Notes	2.3	4.8	7.5	12.6	20.0	30.0
⁸⁹ Y(n, γ)		Experiment ^d	35.64 ^f	29.70	19.83	7.995	1.914	0.1628
	39089.71Y	Calculated ^e	32.63 \pm 1%	28.31 \pm 1%	19.02 \pm 1%	7.960 \pm 1%	1.948 \pm 1%	0.1628 \pm 1%
⁸⁹ Y(n,2n)	39089.71Y	Experiment	398.4	75.69	22.10	5.004	1.054	0.1885
		Calculated	304.6 \pm 0.5%	58.59 \pm 3%	20.92 \pm 22%	4.024 \pm 8%	0.9039 \pm 7%	0.1846 \pm 1%
¹⁹⁷ Au(n, γ)	79197.56C	Experiment	704.7	581.9	455.1	241.6	64.23	5.142
		Calculated	688.5 \pm 1%	613.4 \pm 1%	485.2 \pm 3%	253.1 \pm 3%	69.24 \pm 1%	5.456 \pm 3%
¹⁹⁷ Au(n,2n)	79197.56C	Experiment	1019	193.1	57.70	14.74	3.883	0.898
		Calculated	1165 \pm 0.2%	249.8 \pm 9%	67.60 \pm 5%	17.13 \pm 6%	4.356 \pm 1%	1.024 \pm 1%
²³⁸ U(n, γ)	92238.30Y	Experiment	572.1	470.6	320.0	133.9	73.49	5.747
		Calculated	621.9 \pm 3%	531.8 \pm 3%	365.7 \pm 4%	163.2 \pm 3%	38.75 \pm 3%	3.063 \pm 4%
²³⁸ U(n,2n)	92238.30Y	Experiment	455.5	123.1	41.22	10.90	2.850	0.570
		Calculated	530.2 \pm 2%	125.2 \pm 5%	58.02 \pm 17%	12.14 \pm 1%	3.311 \pm 2%	0.836 \pm 2%
²³⁸ U(n,f)	92238.30Y	Experiment	1794	1053	424.2	67.43	11.47	1.625
		Calculated	1946 \pm 2%	1256 \pm 4%	497.5 \pm 6%	72.93 \pm 2%	12.31 \pm 2%	1.786 \pm 2%
²³⁵ U(n,f)	92235.30Y	Experiment		6087	3226	886.0	190.0	16.47
		Calculated		6769 \pm 1%	3566 \pm 1%	1003 \pm 1%	213.5 \pm 1%	18.65 \pm 1%
¹⁶⁹ Tm(n, γ)	69169.70Y	Experiment		785.6	542.2	309.8	80.70	7.690
		Calculated		968.5 \pm 1%	915.1 \pm 1%	549.0 \pm 1%	145.1 \pm 1%	11.49 \pm 1%
¹⁶⁹ Tm(n,2n)	69169.70Y	Experiment		165.0	47.80	13.95	3.966	0.687
		Calculated		203.8 \pm 4%	92.22 \pm 33%	16.84 \pm 0.4%	4.315 \pm 1%	1.025 \pm 1%
⁹⁰ Zr(n,2n)	40090.26Y	Experiment		48.74	14.47	3.454	0.670	0.120
		Calculated		57.91 \pm 5%	18.23 \pm 6%	3.964 \pm 5%	0.798 \pm 3%	0.181 \pm 1%
⁴⁵ Sc(n, γ)	21045.26Y	Experiment		43.53	34.65	16.31	3.970	0.371
		Calculated		47.03 \pm 3%	39.06 \pm 3%	20.86 \pm 1%	5.110 \pm 1%	0.430 \pm 2%
¹⁹¹ Ir(n, γ)+	77191.70Y	Experiment		1192	1029	539.8	153.6	12.94
		Calculated		653.2 \pm 4%	463.9 \pm 29%	231.5 \pm 6%	61.00 \pm 1%	5.009 \pm 4%
¹⁹³ Ir(n,2n)	77193.71Y	Experiment		160.2	50.96	12.59	3.420	0.787
		Calculated		212.5 \pm 4%	65.06 \pm 6%	16.61 \pm 0.4%	4.219 \pm 1%	1.000 \pm 1%
¹⁹¹ Ir(n, γ)	77193.71Y	Experiment		756.8	696.5	385.3	109.7	7.688
		Calculated		769.8 \pm 1%	672.6 \pm 1%	398.9 \pm 2%	107.9 \pm 1%	8.311 \pm 1%
¹⁹³ Ir(n,n')	77193.71Y	Experiment		999.0	454 \pm 5%	66.10 \pm 10%	7.700 \pm 10%	
		Calculated		3236 \pm 1%	1399 \pm 1%	185.7 \pm 1%	28.61 \pm 1%	
⁵⁸ Ni(n,p)	28058.30Y	Experiment		348.9	138.1	21.17	3.783	0.616
		Calculated		394.2 \pm 2%	152.3 \pm 3%	22.94 \pm 1%	4.151 \pm 1%	0.713 \pm 1%
⁵⁸ Ni(n,2n)	28058.24Y	Experiment		1.505	0.475 \pm 6%	0.110 \pm 6%	0.0200 \pm 10%	0.00590 \pm 33%
		Calculated		2.398 \pm 7%	0.689 \pm 5%	0.159 \pm 0.5%	0.0320 \pm 1%	0.00613 \pm 1%
⁵⁸ Ni(n,d)	28058.24Y	Experiment		47.24	14.37	3.660	0.810	0.160
		Calculated		50.13 \pm 6%	14.43 \pm 5%	3.800 \pm 0.4%	0.882 \pm 1%	0.191 \pm 1%

^aExperimental values taken from Ref. 1.

^bThe number to the left of the decimal is the MCNP nuclide identification number (atomic number followed by mass number). The number to the right of the decimal is the neutron cross section set identifier.

^cActivation cross sections identified by .nnY are described in Ref. 9. Those described by .56C are ENDF/B-V cross sections updated by Los Alamos group T-2 evaluations. Those described by .70Y and .71Y are Los Alamos group T-2 evaluations.

^dExperimentally observed foil activation (activations produced per foil nucleus by 3.815×10^{15} source neutrons).

^eStatistical uncertainties in the calculated values are for one standard deviation.

^fUnless otherwise stated, uncertainties in precision of experimental values are 3%. (See Ref. 1.)

TABLE VIII. Ratio of Observed to Calculated^a Values for Activation of Detector Foils (ENDF/B-V Transport Cross Sections)

Reaction	Activation ^{b,c} Cross Section	Distance from Source (cm)					
		2.3	4.8	7.5	12.6	20.0	30.0
⁸⁹ Y(n,γ)	39089.30Y	1.092 ± 3% ^d	1.048 ± 3%	1.040 ± 3%	1.004 ± 3%	0.982 ± 3%	0.999 ± 3%
⁸⁹ Y(n,2n)	39089.30Y	1.307 ± 6%	1.292 ± 5%	0.946 ± 22%	1.244 ± 9%	1.166 ± 7%	1.021 ± 10%
¹⁹⁷ Au(n,γ)	79197.56C	1.024 ± 3%	0.948 ± 3%	0.937 ± 4%	0.954 ± 5%	0.927 ± 3%	0.942 ± 4%
¹⁹⁷ Au(n,2n)	79197.56C	0.874 ± 3%	0.770 ± 9%	0.853 ± 6%	0.860 ± 6%	0.891 ± 3%	0.870 ± 3%
²³⁸ U(n,γ)	92238.30Y	0.920 ± 4%	0.884 ± 4%	0.870 ± 5%	0.820 ± 4%	1.890 ± 5%	1.870 ± 5%
²³⁸ U(n,2n)	92238.30Y	0.859 ± 3%	0.980 ± 6%	0.710 ± 18%	0.890 ± 3%	0.860 ± 3%	0.682 ± 4%
²³⁸ U(n,f)	92238.30Y	0.922 ± 4%	0.830 ± 5%	0.850 ± 7%	0.932 ± 3%	0.920 ± 3%	0.910 ± 4%
²³⁵ U(n,f)	92235.30Y		0.899 ± 3%	0.900 ± 3%	0.880 ± 3%	0.890 ± 3%	0.880 ± 3%
¹⁶⁹ Tm(n,γ)	69169.70Y		0.811 ± 3%	0.592 ± 3%	0.564 ± 3%	0.550 ± 3%	0.660 ± 3%
¹⁶⁹ Tm(n,2n)	69169.70Y		0.809 ± 5%	0.518 ± 33%	0.828 ± 3%	0.919 ± 3%	0.670 ± 3%
⁹⁰ Zr(n,2n)	40090.26Y		0.841 ± 6%	0.794 ± 6%	0.871 ± 6%	0.839 ± 5%	0.660 ± 3%
⁴⁵ Sc(n,γ)	21045.26Y		0.925 ± 4%	0.887 ± 4%	0.780 ± 3%	0.770 ± 3%	0.862 ± 3%
¹⁹¹ Ir(n,γ)+	77191.70Y		1.824 ± 5%	2.218 ± 29%	2.330 ± 7%	2.518 ± 3%	2.583 ± 5%
¹⁹³ Ir(n,2n)	77193.71Y						
¹⁹¹ Ir(n,2n)	77191.70Y		0.754 ± 5%	0.780 ± 6%	0.758 ± 3%	0.811 ± 3%	0.787 ± 3%
¹⁹³ Ir(n,γ)	77193.71Y		0.983 ± 3%	1.035 ± 3%	1.035 ± 4%	1.016 ± 3%	0.925 ± 3%
¹⁹³ Ir(n,n')	77193.71Y		0.308 ± 3%	0.320 ± 5%	0.356 ± 10%	0.269 ± 10%	
⁵⁸ Ni(n,p)	28058.24Y		0.880 ± 4%	1.102 ± 4%	0.922 ± 3%	0.911 ± 3%	0.864 ± 3%
⁵⁸ Ni(n,2n)	28058.24Y		0.627 ± 7%	0.690 ± 8%	0.733 ± 6%	0.625 ± 10%	0.962 ± 33%
⁵⁸ Ni(n,np)	28058.30Y		0.942 ± 7%	0.990 ± 6%	0.963 ± 3%	0.910 ± 3%	0.830 ± 3%

^aThe neutron transport cross sections used to obtain calculated values are those of ENDF/B-V, as described in the footnote in Section III.A.

^bThe number to the left of the decimal is the MCNP nuclide identification number (atomic number followed by mass number). The number to the right of the decimal is the neutron cross section set identifier.

^cActivation cross sections identified by .nnY are described in Ref. 9. Those described by .56C are ENDF/B-V cross sections updated by Los Alamos group T-2 evaluations. Those described by .70Y and .71Y are Los Alamos group T-2 evaluations.

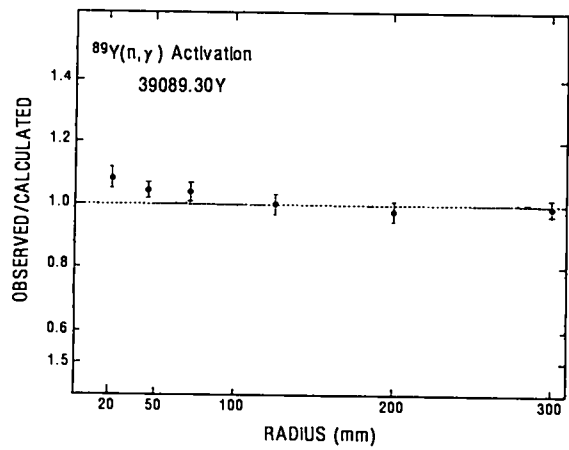
^dThe quoted errors were determined from a square root of the sum of the squares combination of the observed and calculated fractional uncertainties. (No estimates of cross section uncertainties are included.)

The induced background for ampules 340, 341, and 342 was less than 20% of the measured counting rate. Also, the experimental errors were 8-9%. Thus it was possible to obtain acceptable ratios for these three ampules. In Ref. 7, our reanalysis of the ${}^6\text{LiD}$ core experiment, we demonstrated a match between observed and calculated values of tritium production in ${}^7\text{Li}$ to within 6% of unity at all radial experimental positions. If there is any lingering concern over our ability to handle the ${}^7\text{Li}(n,t)$ reaction, the ${}^7\text{Li}$ part of the oralloy core experiment needs to be redone.

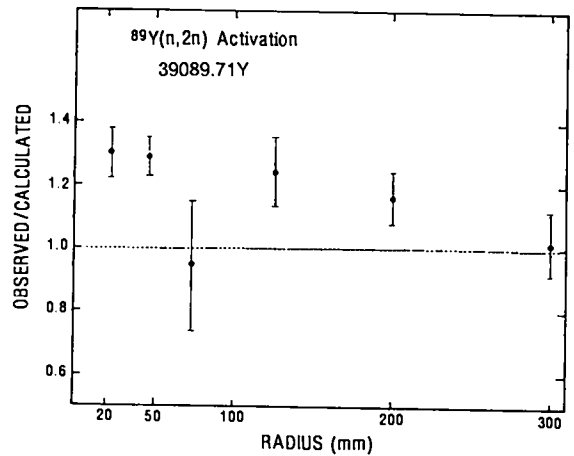
Except for the ${}^7\text{Li}$ experimental problems mentioned above, tritium production from ${}^6\text{Li}$ and ${}^7\text{Li}$ has been wrung out. This should provide stronger confidence in our ability to handle these processes than we have had previously.

ACKNOWLEDGMENTS

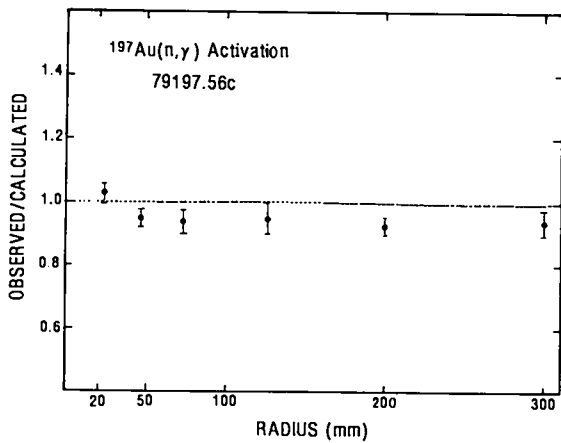
The authors are grateful to Robert Schrandt, Robert Seaman, Robert Little, and Charles Ragan III for their assistance.



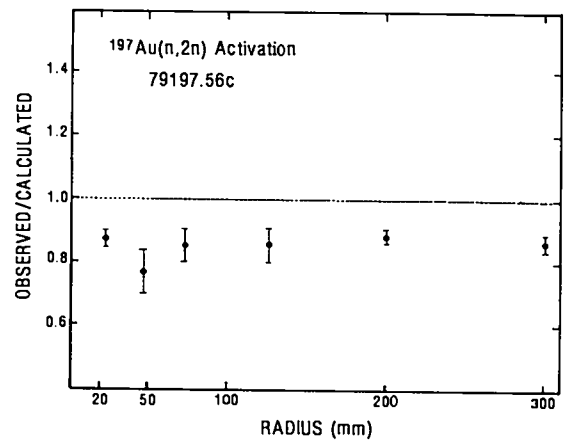
(a)



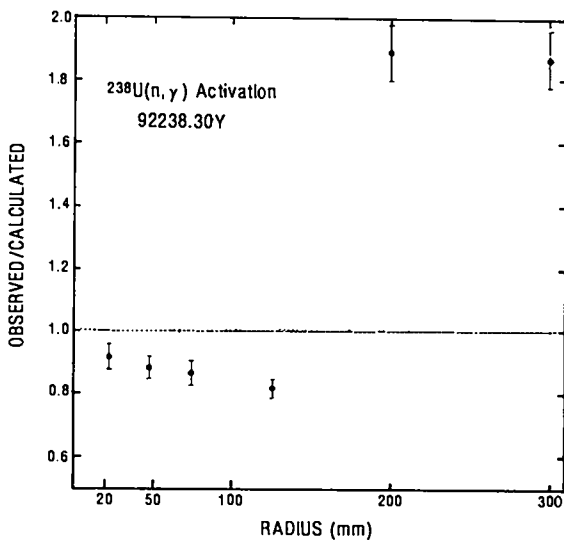
(b)



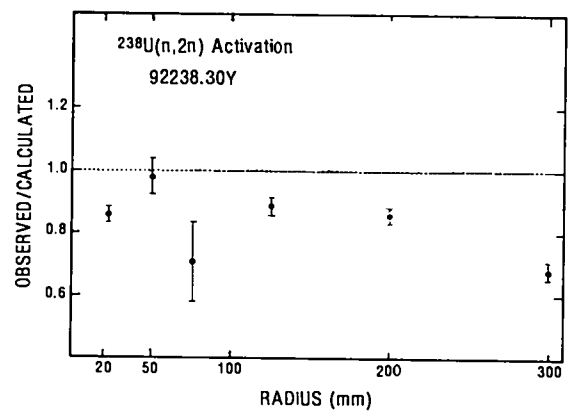
(c)



(d)

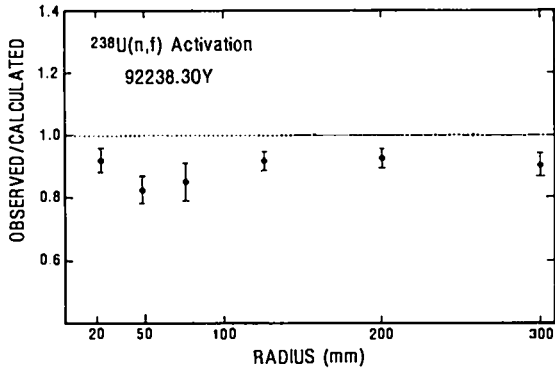


(e)

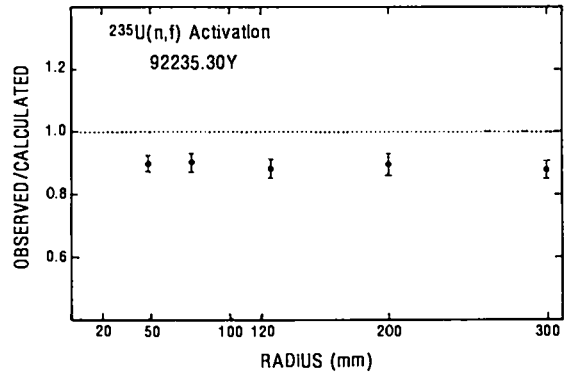


(f)

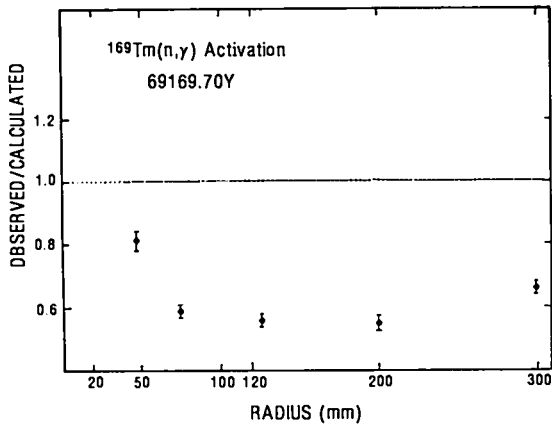
Fig. 4. Ratio of observed-to-calculated activation as a function of foil distance from the center of the assembly.



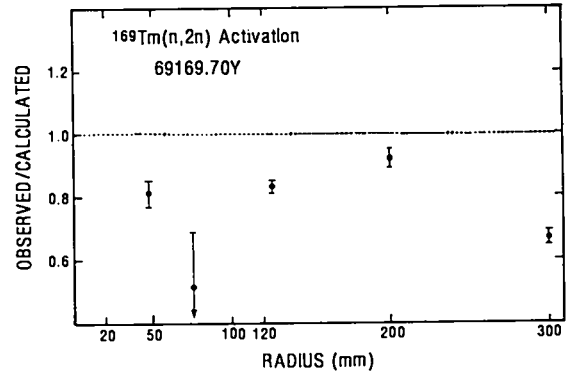
(g)



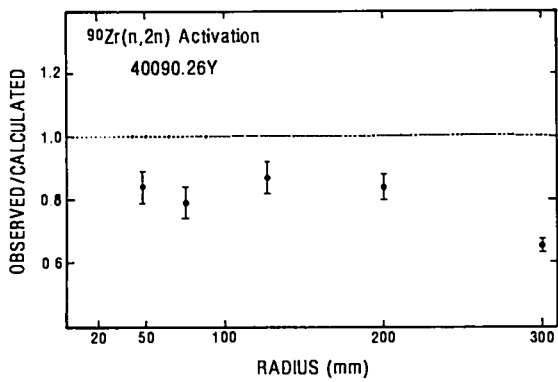
(h)



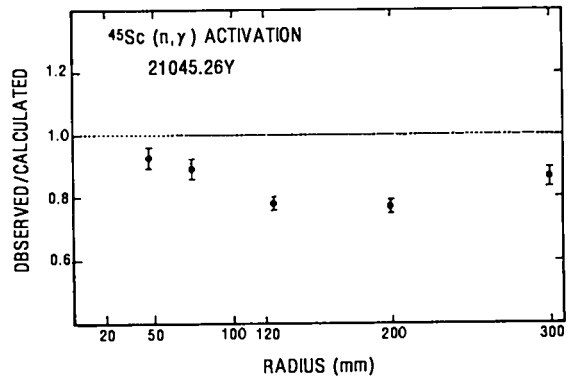
(i)



(j)

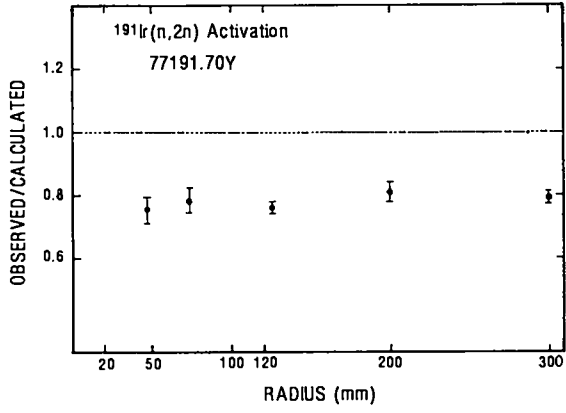


(k)

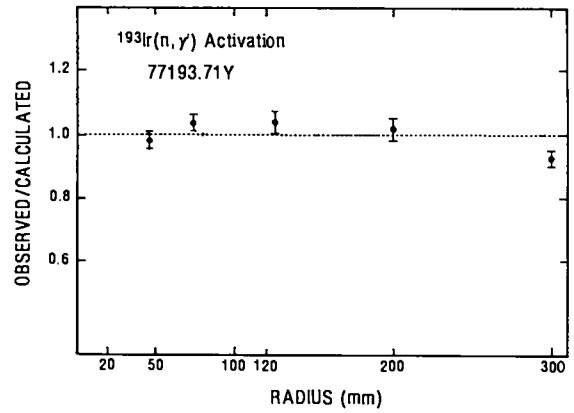


(l)

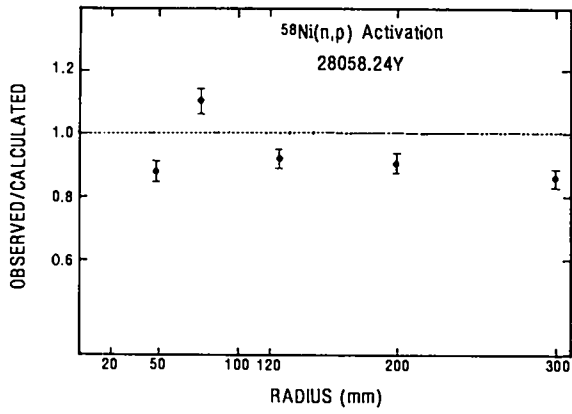
Fig. 4. (Cont.)



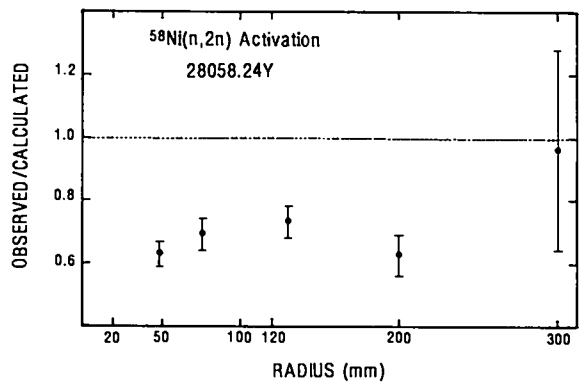
(m)



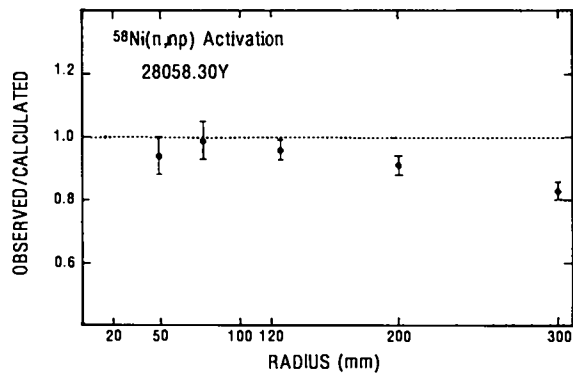
(n)



(o)



(p)



(q)

Fig. 4. (Cont.)

APPENDIX A

IMCNP VERSIIN 8828 07/14/81 9450CP20N2 11 07/24/86 11:34.31
 INP * OYT7CH.B

```

1-      1PITIUM PRODUCTION IN L17H - OY CORE (CHANNELS MODELED)
2-      1 0 -1
3-      2 0 1 -2 -5 22
4-      3 0 1 -3 -6 23
5-      4 0 1 -4 -6 22 23
6-      5 1 -18.6315 1 -5 2 3 4
7-      6 1 -18.6315 5 -6 3 4 7
8-      7 0 6 -7 -8 22
9-      8 4 -0.7300 6 -8 35 39 401 407 408 7 9 11
10-     9 0 6 -8 -9 23
11-    10 4 -0.7396 8 -10 340 341 342 401 407 408 11 13 14
12-    11 0 8 -10 -11 -22 23
13-    12 4 -0.7512 10 -12 340 341 342 348 349 13 15 16
14-    13 0 8 -12 -13 22
15-    14 0 8 -10 -14 23
16-    15 0 10 -12 -15 23
17-    16 0 10 -12 -16 -22 23
18-    17 0 5 -6 -7 22
19-    21 0 12 48 49
20-    35 0 6 -35 335
21-    39 0 6 -39 339
22-    48 2 -8.642 -48 348 12
23-    49 2 -8.642 -49 349 12
24-    52 1 -18.6315 1 -5 -2 -22
25-    53 1 -18.6315 1 -6 -3 -23
26-    54 1 -18.6315 1 -6 -4 22 -23
27-    57 4 -0.7300 6 -7 -8 -22
28-    59 4 -0.7300 6 -8 -9 -23
29-    61 4 -0.7396 6 -10 -11 22 -23
30-    63 4 -0.7512 8 -12 -13 -22
31-    64 4 -0.7396 8 -10 -14 -23
32-    65 4 -0.7512 10 -12 -15 -23
33-    66 4 -0.7512 10 -12 -16 22 -23
34-    67 1 -18.6315 5 -6 -7 -22
35-    335 9 -0.267 -335
36-    339 9 -0.231 -339
37-    340 9 -0.310 -340
38-    341 9 -0.312 -341
39-    342 9 -0.331 -342
40-    348 9 -0.346 -348
41-    349 9 -0.334 -349
42-    401 9 -0.341 -401
43-    407 9 -0.304 -407
44-    408 9 -0.310 -408
45-
46-      1 SO 2.2225
47-      2 CX 0.8500
48-      3 CZ 0.5842
49-      4 1 CX 0.8500
50-      5 SO 4.5860
51-      6 SO 7.61619
52-      7 CX 1.270
53-      8 SO 12.65
54-      9 CZ 0.940
55-     10 SO 20.05
56-     11 1 CX 1.250
57-     12 SO 30.00
58-     13 CX 2.190
59-     14 CZ 1.250
60-     15 CZ 2.830
61-     16 1 CX 2.420
62-     22 PX 0.5
63-     23 PZ 0.5
64-     35 S -5.575 -5.162 2.600 0.7
65-     39 S -4.252 6.701 1.983 0.7
66-     48 S -25.51 -10.24 11.89 0.981
67-     49 S 13.57 25.94 -6.33 0.981
68-     375 S -5.703 -5.281 2.659 0.5
69-     339 S -4.348 6.853 2.027 0.5
70-     340 S -14.81 11.44 6.91 0.9
71-     341 S -17.46 5.16 8.14 0.9
72-     342 S 10.47 -16.51 -4.89 0.9
73-     348 S -25.51 -10.24 11.89 0.9
74-     349 S 13.57 25.94 -6.33 0.9
75-     401 S -9.85 6.28 4.59 0.9
76-     407 S -10.01 -6.38 4.67 0.9
77-     408 S 8.04 8.87 -3.75 0.9
78-
79-      IN 1 10R 2 1 0 0 1 1 0 1 1 4 4 1 GR 0 0 1 3R 2 2R 8 8 1 1 1
80-      NUITE 0
81-      SRC .2 1 .4889 14.13 0 0 0 .5201 14.13 .5105 14.13 0
82-      FILES 14 88SRC
83-      EO 1-3 1-2 1-1 2-1 5-1 1.0 2.0 5.0 10.0 13.0 15.5 20.0
84-      F4 348 349 340 341 342 401 407 408 335 339
85-      FM4 0.3815E-8 7 205
86-      F24 348 349 340 341 342 401 407 408 335 339
87-      M1 92235.50 0.9318 92238.50 0.0582 92234.51 0.0100
88-      M2 48000.51 1.0
89-      M4 1002.55 0.5 3006.50 0.4782 3007.55 0.0218
90-      M6 3006.50 1.0
91-      M7 3007.55 1.0
92-      M8 1001.50 0.5 3006.50 0.4795 3007.55 0.0205
93-      M9 1001.50 0.5 3007.55 0.5
94-      NPS 50000
95-      CTME 400
96-      TOTNU
97-      ERGN 0 20.0
98-      CUTN 1.0E5 0.001 -.8 -.4
99-      PRDNP 25000 25000
100-     FCN 0 19R 1 1 0 12R 1 1 1 1 0 0 0
101-     *TR1 0 0 0 45 90 135 90 0 90 45 90 45
102-

```

APPENDIX B. Comparison of Tritium Production^a in ⁷Li Samples with Cross Sections from ENDF/B-V vs. ENDF/B-V with ²³⁵U Softened Fission Spectrum at High Energy

Sample No.	Location		N(Obs) ^c × 10 ¹³ Experiment (Tritons Produced) / ⁷ Li Atom	N(Calc) × 10 ¹³ ENDF/B-V (Tritons Produced) / ⁷ Li Atom	N(Calc) × 10 ¹³ ENDF/B-V (Modified ²³⁵ U Spectrum ^d) (Tritons Produced) / ⁷ Li Atom	ENDF/B-V	
	r (mm)	ω ^b (deg)				Observed Calculated	(Modified Spectrum) Observed Calculated
348	299.5	-20	0.336 ± 18%	0.378 ± 12%	0.299 ± 13%	0.899 ± 22%	1.12 ± 22%
349	299.5	120	0.328 ± 20%	0.240 ± 13%	0.197 ± 14%	1.367 ± 24%	1.66 ± 24%
340	199.5	35	1.618 ± 8%	1.49 ± 7%	1.17 ± 8%	1.086 ± 11%	1.38 ± 11%
341	199.5	15	1.551 ± 9%	1.84 ± 7%	1.38 ± 8%	0.843 ± 11%	1.12 ± 12%
342	201.5	-125	1.618 ± 9%	1.42 ± 8%	1.06 ± 9%	1.139 ± 12%	1.53 ± 13%
401	125.5	30	9.613 ± 7%	7.42 ± 3%	5.01 ± 4%		
407	127.5	-30	14.71 ± 5%	7.09 ± 3%	4.70 ± 4%		
408	125.5	135	7.41 ± 7%	7.13 ± 3%	4.78 ± 4%		
335	82.2	-40	14.21 ± 14%	30.1 ± 3%	17.1 ± 4%	0.472 ± 14%	0.831 ± 15%
339	83.7	55	14.01 ± 16%	26.7 ± 3%	15.9 ± 4%	0.525 ± 16%	0.881 ± 16%

^aThe quoted uncertainties on both observed and calculated values are for one fractional standard deviation. In addition, there is an estimated <6% systematic error in the observed values which is not included in the errors quoted here.

^bAngles above the parting plane in the experimental configuration are positive; angles below the parting plane are negative.

^cObserved tritium production values were generated from Ref. 1, Table III. (Tritons produced per ⁷Li atom in an ampule from 3.815 × 10¹⁵ source neutrons.)

^dR. C. Little and R. E. Seamon modified the ENDF/B-V ²³⁵U cross section file so that it contained a fission spectrum whose high energy tail at E' = 5.0 MeV was reduced to 50% of that of ENDF/B-IV and at E' = 12 MeV was reduced to 10% of that of ENDF/B-IV. (See Ref. 8.)

APPENDIX C. Comparison of Tritium Production^a in ⁷Li Samples for Induced Background Originating from Ampule Quartz vs. Contaminated Helium

Sample No.	Location		$N(\text{Obs})^c \times 10^{13}$	$N(\text{Obs}) \times 10^{13}$	$N(\text{Calc})^d \times 10^{13}$	Observed ^e	(He Assumed Contaminated) Observed
	r (mm)	ω^b (deg)	$\left(\frac{\text{Tritons Produced}}{^7\text{Li Atom}} \right)$	$\left(\frac{\text{He Assumed Contaminated Tritons Produced}}{^7\text{Li Atom}} \right)$	$\left(\frac{\text{Calculated Tritons Produced}}{^7\text{Li Atom}} \right)$	Calculated	Calculated
348	299.5	-20	0.336 ± 18%	0.343 ± 18%	0.378 ± 12%	0.889 ± 22%	0.907 ± 22%
349	299.5	120	0.328 ± 20%	0.335 ± 20%	0.240 ± 13%	1.367 ± 24%	1.396 ± 24%
340	199.5	35	1.618 ± 8%	1.81 ± 8%	1.49 ± 7%	1.086 ± 11%	1.215 ± 11%
341	199.5	15	1.551 ± 9%	1.74 ± 9%	1.84 ± 7%	0.843 ± 11%	0.946 ± 11%
342	201.5	-125	1.618 ± 9%	1.81 ± 9%	1.42 ± 8%	1.139 ± 12%	1.275 ± 12%
401	125.5	30	9.613 ± 5%	10.22 ± 7%	7.42 ± 3%		
407	127.5	-30	14.71 ± 5%	15.27 ± 5%	7.09 ± 3%		
408	125.5	135	7.41 ± 7%	7.98 ± 7%	7.13 ± 3%		
335	82.2	-40	14.21 ± 14%	23.65 ± 14%	30.1 ± 3%	0.472 ± 14%	0.786 ± 14%
339	83.7	55	14.01 ± 16%	23.42 ± 16%	26.7 ± 3%	0.525 ± 16%	0.877 ± 16%

^aThe quoted uncertainties on both observed and calculated values are for one fractional standard deviation. In addition, there is an estimated <6% systematic error in the observed values which is not included in the errors quoted here.

^bAngles above the parting plane in the experimental configuration are positive; angles below the parting plane are negative.

^cObserved tritium production extracted from Ref. 1, Table III. (Tritons produced per ⁷Li atom in an ampule from 3.815×10^{15} source neutrons.)

^dTritium production calculated using ENDF/B-V - updated where available - cross sections for both transport and tritium production. (Tritons produced per ⁷Li atom in an ampule from 3.815×10^{15} source neutrons.)

^eThe quoted errors were determined from a square root of the sum of the squares combination of the observed and calculated uncertainties.

Appendix D

Comparison of Cross-Section Evaluations

Comparing the foil activation results from Ref. 7 and this report elicits some remarks. It should be noted that in Ref. 7, the principal source of cross-section evaluations for activation reactions was the Barr-Hendricks library based on integral data from activation analysis by INC Division at Los Alamos. With few exceptions, agreement between observed and calculated values is good. Only for $n,2n$ results on ^{90}Zr and ^{191}Ir , and n, γ on ^{169}Tm and ^{45}Sc (a single point only), do the O/C ratios deviate from unity by as much as 20%.

In examining the $n,2n$ results in this paper, we see that except for ^{89}Y all O/C ratios show calculated values that are too high by 15-40%. Uniquely, for ^{89}Y the calculated values are too low by some 20%.

The $n,2n$ evaluations investigated in the calculations in this paper were obtained from ENDF/B-V, Los Alamos Group T-2, and the Lawrence Livermore National Laboratory (LLNL) ACTL library. Those evaluations appear to have been based on microscopic (monoenergetic) cross-section measurements, which can be subject to background problems. Failure to remove all of the experimental background, especially during the rise above the threshold, would result in cross sections that are too large in magnitude; all of the evaluated cross sections (except for ^{89}Y) appear, from our results, too large.

A comparison of the evaluated $n,2n$ cross section for ^{238}U for the Barr-Hendricks and ACTL evaluations is shown in Fig. D-1. Note that the ACTL curve rises more rapidly, to a higher peak, than does the Barr-Hendricks curve. Review of extant microscopic data from the compilation of Garber and Kinsey¹⁰ shows that the ACTL curve indeed follows those measurements. Because of the shape of the neutron spectrum, the difference between the two evaluations between 7 and 10 MeV results in a measurable difference in O/C ratios in these experiments.

The n, γ results from Ref. 7, using Barr-Hendricks evaluations, are generally quite good. Again, the T-2 evaluation of ^{169}Tm and ENDF/B-V for ^{45}Sc gives calculated values that are 20-40% too high. Comparison of the evaluated cross section for ^{45}Sc is shown in Fig. D-2.

It should be noted that in Ref. 7 the ^{238}U n, γ evaluation was modified to fit the measurements of Poenitz,

Fawcett, and Smith,¹¹ which lowered the evaluated curve at high energy. Although the O/C ratios for that reaction in this paper are a bit low at inner foil locations, results for the outer two locations are very large. This appears to be a glitch, as the cross section varies smoothly with neutron energy; the neutron spectrum does not change with foil location sufficiently to produce the observed results.

Of all neutron cross sections, ^{235}U and ^{238}U fission should be well known. ENDF/B-V evaluations gave very good results in Ref. 7; ACTL evaluations gave an O/C ratio some 10% low in this paper for both nuclides at all positions.

Finally, $^{191}\text{Ir}(n, \gamma) + ^{193}\text{Ir}(n, 2n)$ was well represented by the Barr-Hendricks evaluations in Ref. 7. The T-2 evaluations gave O/C ratios off by a factor of 3 in this paper. The $^{193}\text{Ir}(n, n')$ results in Ref. 7 were in good agreement with calculations using the Barr-Hendricks evaluation (with admittedly large uncertainties placed on the evaluated curve). The T-2 evaluation gave O/C ratios off by a factor of 3 in this paper.

In summary, evaluations of activation cross sections based on integral radiochemical data give good results. Evaluations that do not include such data are generally poor.

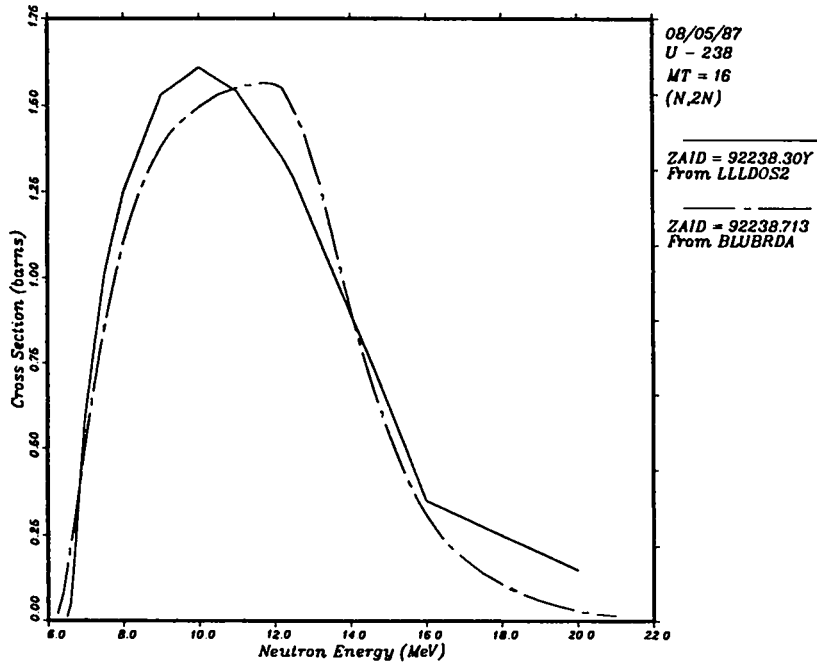


Fig. D-1. Comparison of the evaluated n,2n cross section for ^{238}U for the Barr-Hendricks and ACTL evaluations. Note that the ACTL curve rises more rapidly, to a higher peak, than does the Barr-Hendricks curve.

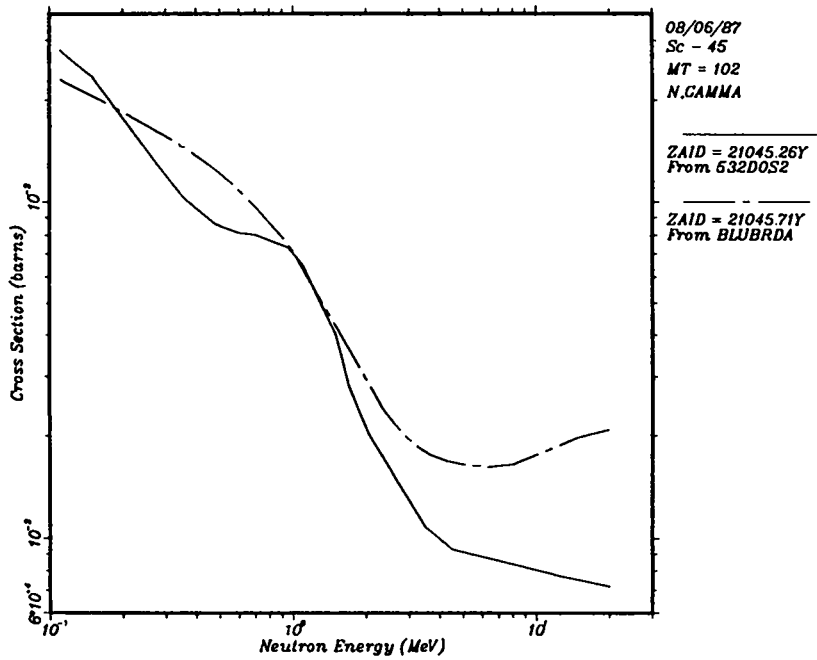


Fig. D-2. Comparison of the evaluated cross section for ^{45}Sc .

REFERENCES

1. A. Hemmendinger, C. E. Ragan, E. R. Shunk, J. M. Anaya, and G. P. Estes, "Tritium Production in Concentric Spheres of ^{235}U and ^6LiD Irradiated by 14-MeV Neutrons," unpublished report, revised May 14, 1979. Available from C. E. Ragan, Los Alamos National Laboratory.
2. J. S. Gilmore, "Report of INC-11 Results on Bluebeard II Sphere Experiment," Los Alamos National Laboratory memorandum INC 11-84-308 (August 1, 1984).
3. A. Hemmendinger, C. E. Ragan, E. R. Shunk, A. N. Ellis, J. M. Anaya, and Jon M. Wallace, "Tritium Production in a Sphere of ^6LiD Irradiated by 14-MeV Neutrons," Los Alamos Scientific Laboratory report LA-7310 (October 1978). An abbreviated form was published in N.S.E. **70**, 274-280, (1979).
4. C. E. Ragan III, G. F. Auchampaugh, A. Hemmendinger, and M. G. Gilbert, "Neutron Spectrum for a Uranium-235 Sphere Bombarded by 14-MeV Neutrons," *Nucl. Sci. Eng.* **61**, 33 (1976).
5. Los Alamos Monte Carlo Group, "MCNP - A General Monte Carlo Code for Neutron and Photon Transport," Los Alamos National Laboratory report LA-7396-M, Rev., Versions 2B and 3A, (April 1981).
6. Los Alamos National Laboratory, "Core," Drawing No. 32Y-20935. Available from L. R. Fawcett, Jr., Los Alamos National Laboratory.
7. L. R. Fawcett, Jr., "Reanalysis of Tritium Production in a Sphere of ^6LiD Irradiated by 14-MeV Neutrons," Los Alamos National Laboratory report LA-10506-MS, (August 1985).
8. R. C. Little and R. E. Seamon, " ^{235}U and ^7Li Cross Sections and Fission Neutron Spectra," Los Alamos National Laboratory memorandum X-6:RES-86-329 (August 7, 1986).
9. R. C. Little and R. E. Seamon, "Dosimetry/Activation Cross Sections for MCNP," Los Alamos National Laboratory memorandum, (March 13, 1984). Available from R. C. Little or R. E. Seamon, Los Alamos National Laboratory.
10. D. I. Garber and R. R. Kinsey, "Neutron Cross Sections: Vol. II, Curves," BNL-325, 3rd Ed., January 1976.
11. W. P. Poenitz, L. R. Fawcett, Jr., and D. L. Smith, "Measurements of the $^{238}\text{U}(n,\gamma)$ Cross Section at Thermal and Fast Neutron Energies," *Nucl. Sci. Eng.* **78**, 239; 1981.

Printed in the United States of America
Available from
National Technical Information Service
US Department of Commerce
5285 Port Royal Road
Springfield, VA 22161

Microfiche (A01)

Page Range	NTIS Price Code						
001-025	A02	151-175	A08	301-325	A14	451-475	A20
026-050	A03	176-200	A09	326-350	A15	476-500	A21
051-075	A04	201-225	A10	351-375	A16	501-525	A22
076-100	A05	226-250	A11	376-400	A17	526-550	A23
101-125	A06	251-275	A12	401-425	A18	551-575	A24
126-150	A07	276-300	A13	426-450	A19	576-600	A25
						601-up*	A99

*Contact NTIS for a price quote.

